COMPTES RENDUS

CHIMIE

Full paper / Mémoire

Electrocatalysis of hydrogen evolution by synthetic diiron units using weak acids as the proton source: Pathways of doubtful relevance to enzymic catalysis by the diiron subsite of [FeFe] hydrogenase

Stacey J. Borg [a], Saad K. Ibrahim [b], Christopher J. Pickett [b,*], Stephen P. Best [a,*]

[a] *School of Chemistry, University of Melbourne, Melbourne 3010, Victoria, Australia*
[b] *School of Chemical Sciences and Pharmacy, University of East Anglia, Norwich NR4 7TJ, UK*

Abstract

IR spectroelectrochemical studies of bis(thiolate) and dithiolate-bridged diiron carbonyl compounds, $[Fe_2(\mu\text{-}SR)_2(CO)_6]$, show that the primary reduction process results in rapid chemical reaction, leading to two-electron reduced products. When the reaction is conducted under an inert atmosphere, the major product is $[Fe_2(\mu\text{-}SR)(\mu\text{-}CO)(CO)_6]^{1-}$, where in the case of dithiolate-bridged neutral compounds the product has one bridging and one non-bound sulfur atom. This product is formed in near-quantitative yield for solutions saturated with CO. Reduction of $[Fe_2(\mu\text{-}SR)(\mu\text{-}CO)(CO)_6]^{1-}$ occurs at potentials near -2.0 V vs. SCE to give a range of products including $[Fe(CO)_4]^{2-}$. Reduction of thiolate-bridged diiron compounds at mild potentials in the presence of CH_3COOH leads to formation of $[Fe_2(\mu\text{-}SR)(\mu\text{-}CO)(CO)_6]^{1-}$ and this is accompanied by an acid-base reaction with the dissociated thiolate. The reaction is largely reversible with recovery of *ca*. 90% of the starting diiron compound and CH_3COOH. In the presence of acid, reduction of $[Fe_2(\mu\text{-}SR)_2(CO)_6]$ proceeds without generation of observable concentrations of the structurally related one-electron reduced compound. Electrocatalytic proton reduction is achieved when the potential is stepped sufficiently negative to reduce $[Fe_2(\mu\text{-}SR)(\mu\text{-}CO)(CO)_6]^{1-}$, an observation in keeping with the cyclic voltammetry of the system. Since the catalytic species involved in the weak-acid reactions is structurally distinct from the starting material, and the diiron subsite of the hydrogenase H-cluster, these experiments are of dubious relevance to the biological system. ***To cite this article: S. J. Borg et al., C. R. Chimie 11 (2008).***
© 2008 Académie des sciences. Published by Elsevier Masson SAS. All rights reserved.

Keywords: Transition metal carbonyls; Spectroelectrochemistry; Electrocatalysis; IR spectroscopy; [FeFe] hydrogenase

1. Introduction

The comparative explosion in the chemistry of dithiolate-bridged diiron carbonyls and their variously substituted analogues is, of course, driven by the hope that compounds related to the diiron subsite of the [FeFe] hydrogenase H-cluster, $\{2Fe\}_H$, will provide the efficient catalysts needed for either production or consumption of dihydrogen. Well-defined electrocatalytic responses have been reported for many of these compounds [1] and an important goal of the chemical studies is the identification of

* Corresponding authors.
E-mail addresses: c.pickett@uea.ac.uk (C.J. Pickett), spbest@unimelb.edu.au (S.P. Best).

materials that support rapid electrocatalysis at relatively modest overpotentials.

Rational catalyst design and optimisation is underpinned by an understanding of the reaction path. For the dithiolate-bridged diiron carbonyl compounds related to {2Fe}$_H$ electrocatalysis has been studied in most detail for Fe$_2$(S(CH$_2$)$_3$S)(CO)$_6$ (**3S**) [2,3]. Electrochemical and spectroelectrochemical (SEC) studies of electrocatalytic proton reduction of *p*-toluene sulfonic acid (HOTs) by **3S** suggest a reaction path that involves a sequence of two one-electron, one-proton steps to give a two-electron, two-proton product that undergoes dihydrogen elimination. The relatively slow rate of dihydrogen elimination (*ca.* 5 s^{-1}) is increased by further reduction [2,3]. Comparison between the reduction chemistry and electrocatalysis by **3S** and phosphido-bridged analogues suggests that the reaction path for the two-electron, two-proton reaction involves hydrides that occupy sites opposite to the S (or P) bridging ligand [4]. The molecular details of the reaction have been explored by density functional theoretical (DFT) methods [5]. These studies support the proposed sequence of reduction and protonation reactions and the proposition that dihydrogen elimination from the two-electron, two-proton product of **3S** is slow and rate limiting [2]. Importantly, when taken together with studies of the phosphido-bridged analogues [4,6], this work provided the first experimental evidence supporting the proposition that the reaction path involves protonation of the Fe–Fe bond. Whereas HOTs is a sufficiently strong acid to protonate **3S**$^-$ (in CH$_3$CN and THF), under the same conditions acetic acid (HOAc) is not a strong enough acid to protonate the one-electron reduced product and the reaction path for electrocatalysis by weak acids such as HOAc has been suggested to proceed through two one-electron reductions followed by two protonation steps [7]. Contrary to the general observation of one-electron reduction steps for bis(thiolate) and dithiolate-bridged diiron carbonyl compounds, the benzene-1,2-dithiolate analogue (**BDT**) undergoes a reversible two-electron reduction [8,9]. Very recent electrochemical and DFT studies of the electrocatalytic proton reduction reaction of HOAc with **BDT** have revealed that the reaction proceeds with significant structural reorganisation following two-electron reduction and it is at this level that the first protonation step occurs; further reduction and protonation lead to dihydrogen elimination [10].

Two issues related to electrocatalytic proton reduction have been raised by Evans and coworkers [11]. The first concerns the impact of direct proton reduction on the electrocatalytic response, a matter particularly important when a significant rate of reaction occurs with a high overpotential. Under these circumstances the choice of electrode material is of critical importance. For electrocatalytic proton reduction the overpotential presented by a mercury electrode would, in the absence of complicating chemistry, present the best choice. Owing to the high affinity of mercury for thiolates alternative working electrode materials need to be used for the study of H-cluster analogues and vitreous carbon presents a suitable alternative. The second issue concerns the impact of the acid strength (pK_a) on the driving force for the reaction. Since the potential needed for an electrocatalytic reaction that follows an EC$'$ path (electrochemical then chemical steps preceding reaction to recover the starting complex) is largely determined by the redox potential of the catalyst, the overpotential will be lowest for electrocatalytic proton reduction by the weakest acid capable of supporting the reaction at a given rate.

The only substantive operational reason for using a relatively weak acid in a functional system is to avoid irreversible destruction of the catalytic material or, if supported, the synthetic or biological matrix in which it is contained. Probing mechanism and/or suppressing uncatalysed reaction pathways by using weak acids can be informative and many studies report experiments of this type that have been used to benchmark the activity of the newly reported compounds [7,12–18]. In this contribution we show that for a diverse range of thiolate-bridged diiron carbonyl compounds reduction gives stable products with a grossly different structure from that of the parent compound and that electrocatalysis of proton reduction with a weak acid source such as HOAc proceeds after further reduction of these structurally altered species. For this reason such experiments provide a poor and misleading criterion for relating the electrocatalytic activity to the structure and composition of the diiron parent compound and the relationship this may have to the diiron subsite of [FeFe] hydrogenase.

2. Results and discussion

When dealing with aqueous media the definition of "weak" and "strong" acids is well understood, however the application of these terms in the context of nonaqueous media is often ambiguous and requires qualification. In acetonitrile only acids such as triflic and perchloric acids are largely dissociated and *p*-toluene sulfonic acid (HOTs) with a pK_a of *ca.* 8 is overwhelmingly in the undissociated form [19]. In

the context of the electrocatalytic proton reduction reactions of bridged diiron(I) carbonyl compounds at the focus of this study "weak" and "strong" acids are operationally defined in terms of their ability to protonate the one-electron reduced form of the compound. In terms of this operational definition HOTs is an example of a strong acid and HOAc is a weak acid.

The influence of weak and strong acids on the reduction chemistry of dithiolate-bridged diiron hexacarbonyl compounds is illustrated by the electrocatalytic and IR spectroelectrochemical (IR-SEC) properties of the ethylene (**2S**) and propylene (**3S**) linked dithiolates and the bis(thiolate) compound $Fe_2(\mu\text{-SEt})_2(CO)_6$, **SEt**. The inclusion of **SEt** allows consideration of the case where rearrangement or partial dissociation of the dithiolate is more facile. The electrochemical properties of thiolate-bridged diiron carbonyl compounds have been examined by several workers and the cyclic voltammograms of the three compounds are shown in Fig. 1 [20,21]. The primary reduction wave (process I) is, at best, partly reversible for the dithiolates and is irreversible for the bis(thiolate) compounds. Process I is nearly reversible for CO-saturated solutions of **2S** and **3S** and this suggests a reaction path involving CO dissociation. A second reduction wave (process II) is most clearly defined for **SEt**; for **3S** and **2S** the peak current is less than half of that obtained for process I. In all three cases at least two different reductions can be discerned for processes II. The daughter products formed following reduction differ both in terms of their relative concentrations and re-oxidation potentials. It is noteworthy

that there is a surprisingly large difference between the re-oxidation potentials for the daughter products of **2S** and **3S**.

The reduction chemistry of **3S** has been shown to feature an unexpectedly rich chemistry that involves rearrangement of the CO and thiolato groups as well as unexpected dimeric (tetrairon) forms [2], some of which have been characterised by X-ray crystallography [22,23]. The reactivity and structure of the different species may be understood in terms of the strong tendency of the Fe centres to maintain a so-called "18 electron" configuration [24]. Unlike the analogous phosphido-bridged compounds, which undergo two-electron reduction reactions to yield electron precise electron configurations simply by the loss of the Fe−Fe bond [4], the thiolate-bridged compounds predominantly undergo reduction in one-electron steps. The chemical reversibility of process I is sensitive to the identity of the bridging ligand, generally being greater for dithiolates than for bis thiolates, and this is evident from the voltammetry shown in Fig. 1. Clearly a reaction path involving CO loss is implicated by these observations, however, the CO-depleted reduced species initially formed have not been identified. IR spectroelectrochemical (IR-SEC) studies of **3S** suggest that reaction of **3S**$^{1-}$ is fast relative to reduction at the electrode and the lifetime of the one-electron reduced product is inversely proportional to the concentration of **3S**, suggesting a bimolecular reaction path [2]. Since CO dissociation from the one-electron reduced product would formally give an electron deficient species the involvement of a second such species would provide a path to a decarbonylated electron precise product. While the suggested structures of the singly decarbonylated tetrairon species shown in Scheme 1 are speculative it has recently been shown that one-electron reduction of the related compounds, $Fe_2(\mu\text{-pdt})(CO)_5L$, where L is a labile ligand, yields a tetrairon species (**2S$_D$**) with two bridging CO ligands, which has been characterised by X-ray crystallography (Scheme 1) [23]. The studies of **2S$_D$** demonstrate that rearrangement between the diiron and tetrairon species may be fast on the electrochemical timescale. It is likely that the differing stabilities of the tetrairon species for ethanedithiolate and propanedithiolate compounds serves as an important factor in explaining the differing reaction pathways obtained during reduction of **2S** and **3S**.

The electrochemistry of **3S** in the presence of HOTs has been reported and the reaction path considered in detail [2]. The electrocatalytic response of **2S** with HOTs is given in Fig. 2a. Protonation of the one-electron
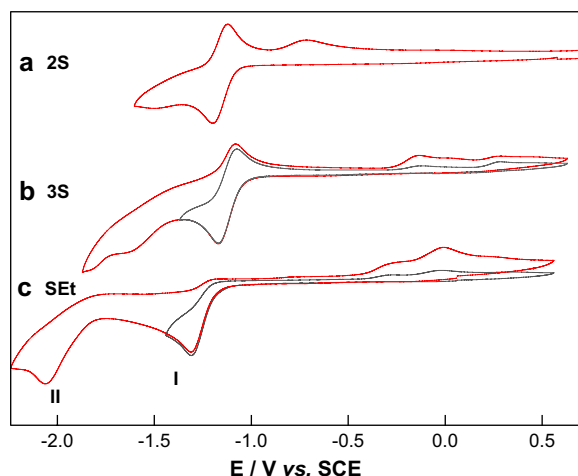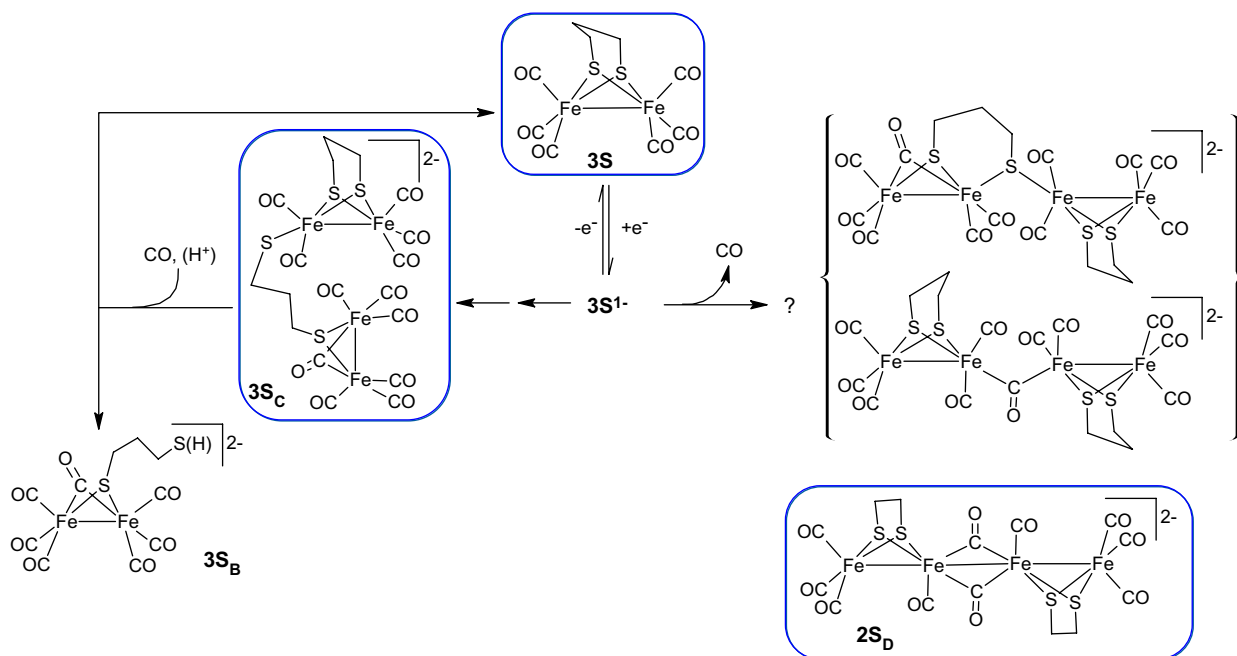

Fig. 1. Cyclic voltammetry of 1 mM solutions of (a) **2S**, (b) **3S** and (c) **SEt** in THF (0.2 M TBA[PF$_6$], vitreous carbon working electrode, scan rate 100 mV s^{-1}).

Scheme 1. X-ray structures are available for **3S** [25], **3S$_C$** [22] and **3S$_D$** [23].

product is reflected by a shift of process I to more positive potentials where the magnitude of the shift is related to the magnitude of the equilibrium and rate constants. Electrochemical simulation has shown that an electrocatalytic pathway involving two one-electron reduction/protonation sequences (ECEC′ reaction) satisfactorily accounts for the process occurring at more positive potentials [2] and a simulation based on the scheme given in Ref. [2] is shown in Fig. 2b. The rate limiting step, dihydrogen elimination from H$_2$**3S**, may be accelerated by further reduction and this accounts for a second process occurring at slightly more negative potentials at higher acid concentrations. DFT calculations suggest that such a reaction path is energetically feasible and also provide insights into the structures of the reduced species [5].

The involvement of tetrairon species in the electrocatalytic reaction is reflected by the differing effects of CO on the reduction chemistry of **2S** and **3S** [2,26]. Whereas additional CO improves the reversibility of process I, by eliminating formation of decarbonylated products, in the presence of acid CO addition to the tetrairon species **3S$_C$** is sufficiently rapid to compete with electrocatalysis (Scheme 1). It is important to note that electrocatalytic proton reduction by **2S** is not inhibited by CO and this has been explained in terms of the different tetrairon product formed following reduction [26].

A strong electrocatalytic response is obtained for solutions of HOAc with a wide range of hydrogenase model compounds, where the results obtained for **SEt** are given in Fig. 2c. Since **SEt^{1-}** is not protonated by HOAc there is no shift of the potential of process I to more positive values. While the main electrocatalytic wave appears to be associated with process II additional waves develop at potentials intermediate between processes I and II. The background current due to direct reduction of HOAc at the carbon electrode makes a negligible contribution to the response at potentials more positive than -1.9 V and contributes less than 10% of the current at -2.2 V. As noted by Evans and coworkers the redox potential for the reduction of the respective acids depends on their pK_a and for acetonitrile solutions the E^0_{HA} value of HOTs is 0.71 V more positive than that of HOAc [11]. Consequently, the overpotential for reduction of the acid is lower for the reactions with HOAc.

A key question that has largely been avoided in previous studies of electrocatalytic proton reduction of weak acids by hydrogenase model compounds is the form of the catalytic species responsible for the reaction. Superficially the assignment of the two reduction waves of **SEt** to sequential electron transfer reactions and thus formation of **SEt^{2-}** leads to an electrocatalytic sequence in which dihydrogen elimination follows two protonation steps (EECC′ reaction). While
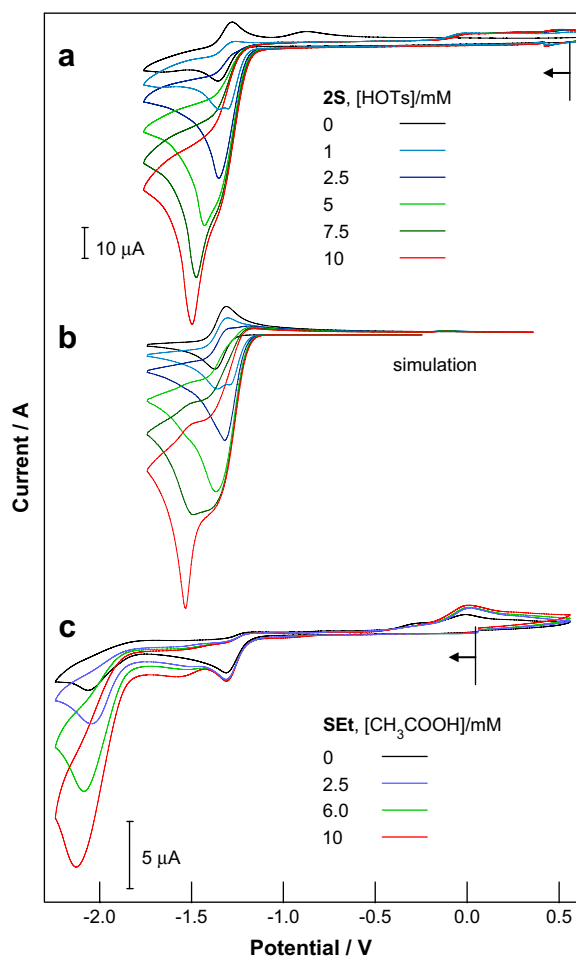
Fig. 2. Electrocatalytic proton reduction by **2S** and **SEt**. Cyclic voltammetry of (a) **2S** (1 mM) and HOTs (0–10 mM); (b) digital simulation based on the electrocatalytic scheme described in Ref. [2]; (c) **SEt** (1 mM) and HOAc (0–10 mM). Experimental data were obtained from THF solutions with 0.2 M TBA[PF$_6$] as supporting electrolyte and either a 1 mm (**SEt**) or 2 mm (**2S**) diameter vitreous carbon working electrode at a scan rate of 100 mV s^{-1}.

studies of electrocatalytic proton reduction of HOAc by hydrogenase model compounds commonly assign EECC′ reaction paths, several aspects of the voltammetry sit uncomfortably with such an assignment. The most important of these is the attribution of process II to the **Complex^{1-}/Complex^{2-}** couple. In simple terms the irreversibility of the **SEt/SEt^{1-}** couple would suggest that process II is due to chemically altered reduced species, moreover comparison between the electrochemistry of bis thiolate- and dithiolate-bridged compounds shows that the value of I_{pc} for process II is not related to the reversibility of process I. A recent detailed study by Capon et al. demonstrates clearly that while the primary reduction wave of thiolate-bridged

diiron compounds related to **3S** has many of the characteristics of a one-electron process, the second reduction is also involved [27]. In these cases the electrochemistry is complicated by competing chemical reactions and a slow rate of heterogeneous electron transfer. It was shown that observation of a distinct electrochemical response for the two redox waves requires the collection of voltammograms at scan speeds greater than 0.5 V s^{-1} and in these cases the second reduction occurs *ca.* 0.2 V more negative than the first [27].

The details of the chemical species formed during the course of the redox reaction are most clearly delineated by recourse to spectroscopy. Currently IR-SEC studies are available for the reduction of **2S** and **3S** [2,18]. The extension of these studies to **SEt** is important given the relative prominence of process II. The initial phase (4 s) of reduction of **SEt** at a potential encompassing the first reduction wave (−1.4 V) leads to the depletion of the starting material (negative bands at 2073, 2036 and 1994 cm^{-1}) and its conversion into new species with ν(CO) bands at 2018, 2014, 1974, 1952, 1941, 1925, 1888, and 1728 cm^{-1} (Fig. 3a). At longer times an additional low intensity ν(CO) band grows into the spectrum near 1870 cm^{-1}. When the potential is then set to less negative values (−1 V) there is partial recovery of **SEt** (10−15%) and this is associated with the depletion of a subset of the growth bands (Fig. 3b). The remaining set of growth bands has a profile that closely resembles the spectrum of a previously characterised product with bridging thiolate and CO groups, **3S$_B$** (Scheme 1). On this basis a product with a similar structure, **SEt$_B$**, is formed following reduction of **SEt**. This assignment is confirmed by observation of the EPR spectrum of the oxidised form of **SEt$_B$** [28]. Application of potentials more positive than +0.2 V results in oxidation of **SEt$_B$** with formation of **SEt** (Fig. 3c). The recovery of **SEt** (*ca.* 75%) following reduction−oxidation cycle is poorer than that for the analogous dithiolate-bridged compounds **2S** and **3S** [2,18], and the final spectra (Fig. 3c) include broad bands near 2080, 2105 and 1980 cm^{-1} due to unidentified reaction products. It is important to note that at no stage through the reductions are bands attributable to the one-electron reduced product of **SEt** evident in the spectra. This observation is consistent with the irreversible character of process I for **SEt**.

Application of a reducing potential to a solution of **SEt** sufficient to access process II results in a more complicated set of time dependent spectral changes (Fig. 4a). Coincident with the depletion of **SEt** there is an immediate growth of a set of bands attributable
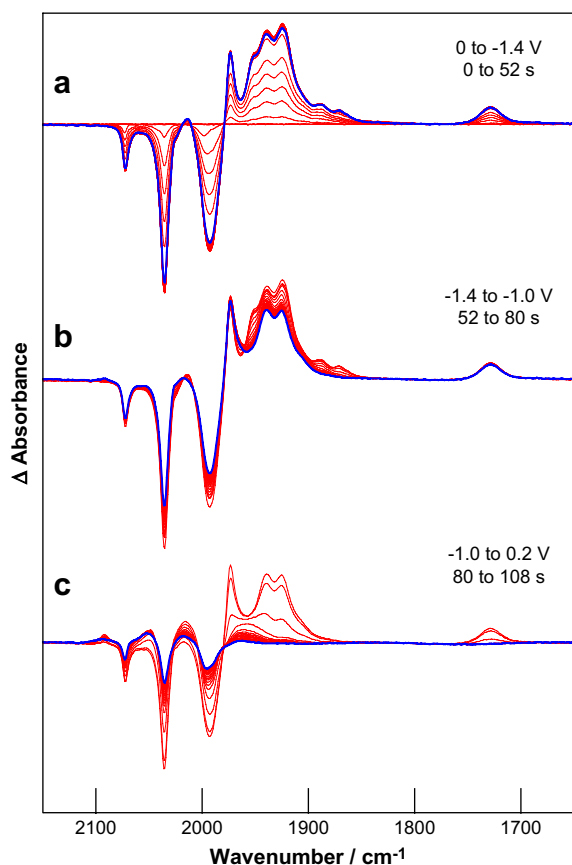
Fig. 3. Differential absorption IR-SEC spectra of **SEt** (1 mM, 0.1 M TBA[ClO$_4$], CH$_3$CN, Ar) during (a) reduction through process I, (b) re-oxidation at mild potentials and (c) re-oxidation at +0.2 V. The last spectrum of each group is highlighted.
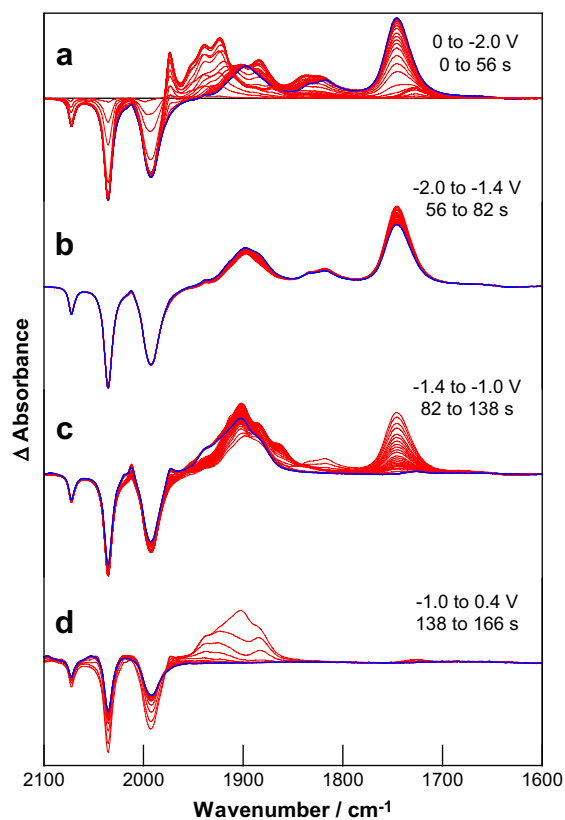

Fig. 4. Differential absorption IR-SEC spectra of **SEt** (same solution as for Fig. 3) during (a) reduction through process II and re-oxidation at (b) −1.4 V, (c) −1.0 V and (d) +0.4 V. The last spectrum of each group is highlighted.

to **SEt$_B$**, however, this species is unstable at the applied potential and the intensity of the growth bands decays to give a final spectrum with weak bands near 1900 and 1820 cm^{-1} and a strong band at 1745 cm^{-1}. Re-oxidation at mild potentials results in depletion of the band at 1745 cm^{-1} with minimal recovery of **SEt** and a set of broad bands centred on 1900 cm^{-1} (Fig. 4b,c). Re-oxidation at more positive potentials (+0.4 V) results in recovery of about 30% of the starting material leaving weak residual growth bands between 2050 and 2000 cm^{-1} (Fig. 4d). Clearly the reduction of **SEt$_B$** is associated with process II where the irreversibility of the spectral changes is consistent with the irreversible electrochemical behaviour. The main reduction product of the reaction is tetracarbonyl ferrate, [Fe(CO)$_4$]$^{2-}$, a common product formed following reductive degradation of iron carbonyl complexes [29,30]. The assignment of the band at 1745 cm^{-1} to this species is confirmed in experiments conducted using CO saturated solutions. In this case

there is a simpler distribution of products and the re-oxidation process proceeds with the observation of bands at 1913, 1887 and 1866 cm^{-1} which are consistent with the formation of [Fe$_2$(CO)$_8$]$^{2-}$ [28].

The spectral changes obtained following reduction of **3S** in the presence of HOAc at potentials sufficient to access process I are shown in Fig. 5 and at potentials sufficient to access process II in Fig. 6. Under mild conditions the reaction proceeds to give similar products in the presence and absence of HOAc and the primary reduction product is **3S$_B$**. Despite the greater relative stability of **3S^{1-}** over **SEt^{1-}** there is no sign of formation of **3S^{1-}** during the early stage of the reaction (Fig. 5a). In the absence of additional CO other reduction products are generated in low concentration and this is reflected by the features apparent in the spectra at 1900 and 1955 cm^{-1}. It is interesting to note that during the formation of **3S$_B$** there is depletion of bands due to HOAc at 1730 and 1755 cm^{-1}. Once the electrosynthesis in the thin layer of solution
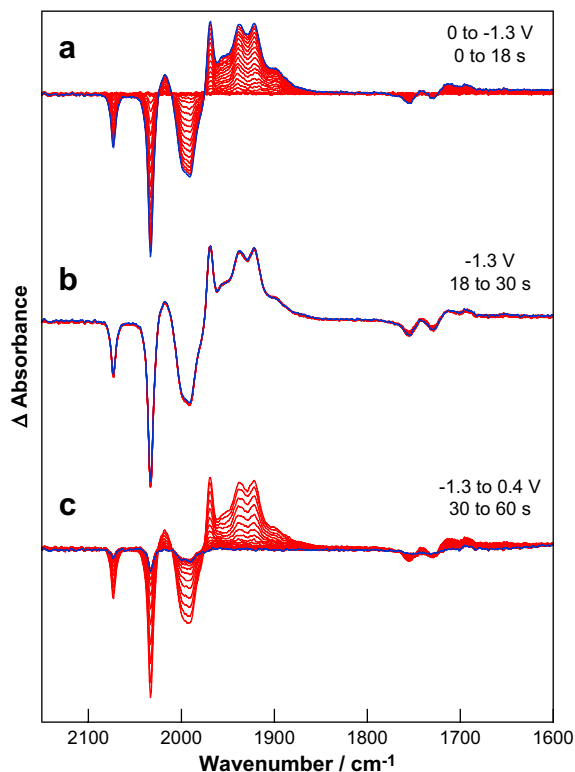
Fig. 5. Differential absorption IR-SEC spectra of a solution of **3S** (1 mM) and HOAc (20 mM) in THF (0.2 M TBA[PF$_6$]) during (a) reduction (process I), (b) time dependent changes following reduction and (c) re-oxidation at 0.4 V. The last spectrum of each group is highlighted.
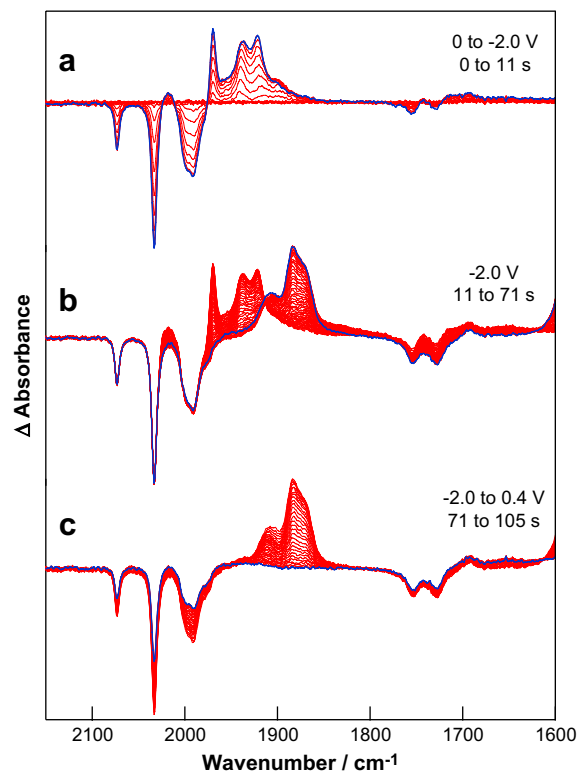
Fig. 6. Differential absorption IR-SEC spectra of the solution of **3S** used for Fig. 5 during (a) reduction (process II), (b) time dependent changes following reduction and (c) re-oxidation at 0.4 V. The last spectrum of each group is highlighted.

between the working electrode and the IR-transmitting window is complete there is no further depletion of HOAc (Fig. 5b). Application of a re-oxidising potential (+0.5 V) results in substantial (>90%) recovery of **3S** together with near-quantitative recovery of HOAc (Fig. 5c). The reversible interconversion of HOAc and OAc^{1-} is due to an acid-base reaction with the dissociated thiolate formed during generation of **3S$_B$** (Scheme 1).

Experiments conducted with an applied potential sufficient to access process II give spectral changes corresponding to the reduction of **3S** to give **3S$_B$** as the initial product (Fig. 6a). Following exhaustive depletion of the neutral compound, **3S$_B$** is replaced by more highly reduced products with bands at 1907, 1883, 1871 cm^{-1} in the ν(CO) region together with bands at 1590 and 1373 cm^{-1} (Fig. 6b). Through this period there is continued depletion of HOAc. Application of a potential of +0.5 V is accompanied by the loss of the growth features together with recovery of *ca.* 40% of the neutral compound and partial recovery of HOAc (Fig. 6c). The generation of dihydrogen

during the reduction process is implied by the relative magnitudes of the depletion bands due to **3S** and HOAc, together with the diminished extent of recovery of HOAc during re-oxidation. While it is not possible at this stage to comment on the form of the highly reduced species the low wavenumber features are consistent with the protonation of highly reduced metal carbonyl species to give formyl adducts. While these experiments do not allow identification of the catalytic species, it is clear, however, that reduction beyond **3S$_B$** is required in order to achieve proton reduction.

3. Conclusion

Consideration of the electrochemical response of bis(thiolate) and dithiolate-bridged diiron carbonyl compounds casts grave doubt on the simple EECC′ electrocatalytic path most commonly quoted for reactions where weak acids are involved. The rapid scan voltammetry reported by Capon et al. [27] would suggest that had such a scheme applied then the purportedly active two-electron reduced species would be

formed at potentials more positive than process II. This conclusion is further supported by analysis of the electrocatalytic reduction of HOAc by **BDT** [10], a complex exhibiting a reversible two-electron couple [8,9]. The IR-SEC results reported herein confirm that reduction of the neutral bis thiolate (**SEt**) and dithiolate (**2S** and **3S**) bridged diiron(I) carbonyl compounds at mild potentials (process I) generates species analogous to **3S_B** (Scheme 1) and the course of this reaction is not altered by the presence of HOAc. Process II does not correspond to the **Complex^{1−}/Complex^{2−}** couple but is associated with reduction of species analogous to **3S_B**. In the absence of additional CO the stoichiometry of the reaction demands formation of additional iron-based products and these also may contribute to the electrocatalytic response. It is important to note that while the catalysts are interesting in their own right, the structure of the electrocatalytic species is more likely to be related to **3S_B** than **3S** and it is therefore highly unlikely that this chemistry is related to that of the H-cluster. If the purpose of the study of the electrocatalytic reactions of H-cluster model compounds is to cast light on the reaction chemistry of the biological system then reactions involving weak acids are at best of dubious value since there is no basis for assignment of the structure of the electrocatalytic species. Paradoxically, the reaction is less complicated when strong acids are used since in this case protonation of the one-electron reduced product engages a reaction path which, according to DFT calculations [5], leads to dihydrogen elimination from dithiolate (or bis thiolate) bridged diiron compounds.

4. Experimental

Unless otherwise stated chemicals (Aldrich) and high-purity gases (BOC) were obtained from commercial sources and used without further purification. The diiron hexacarbonyl compounds $Fe_2(\mu\text{-}S(CH_2)_2S)(CO)_6$ **2S**, $Fe_2(\mu\text{-}S(CH_2)_3S)(CO)_6$ **3S** and $Fe_2(\mu\text{-}SEt)_2(CO)_6$ **SEt**, were prepared by literature methods [31], and confirmed to be pure by spectroscopic and electrochemical analyses. All manipulations of solutions used in SEC measurements were carried out under a dinitrogen or argon atmosphere using standard Schlenk techniques or through the use of a VAC glovebox. Tetrahydrofuran (HPLC grade) was filtered through activated neutral aluminium oxide (Brockmann I, 150 mesh, Aldrich) to remove peroxides and pre-dry, then distilled from sodium benzophenone ketyl [32]. Acetonitrile was distilled over calcium hydride. Tetra-*n*-butylammonium perchlorate (TBA[ClO₄]) and tetra-

n-butylammonium hexafluorophosphate (TBA[PF₆]), used as supporting electrolytes, were prepared and purified using standard procedures [33]. ***Caution! Perchlorate salts are potentially explosive. Solutions containing TBA[ClO₄] as a supporting electrolyte should not be allowed to evaporate to dryness.***

Cyclic voltammetry experiments were controlled using an Autolab PGSTAT30 potentiostat with GPES software and were carried out in a one-compartment glass cell using a 1 mm diameter vitreous carbon working, platinum counter, and jacketed silver wire reference electrodes. Spectroelectrochemical (SEC) experiments were conducted using a purpose built cell previously described [34], and employed a 3 mm diameter vitreous carbon working electrode, silver pseudoreference electrode, and platinum foil counter electrode. The potential of the reference electrode was estimated from the voltammetry of the solution under investigation and, by comparison with experiments conducted in the presence of ferrocene (Fc), all potentials are quoted relative to the Ag/AgCl reference electrode. Against this reference the Fc⁺/Fc couple occurs at +0.51 V in CH_2Cl_2 [35,36]. The applied potential was controlled using a PAR model 362 potentiostat. A Powerlab 4/20 interface (ADInstruments) using EChem V1.5.2 or Chart V4.12 provided a means of setting the applied potential and monitoring the potential and current responses during SEC experiments. Digital simulation of the voltammetry was conducted using the program DigiElch (version 4, DigiSoft) [37−39].

IR spectra were obtained using a Bio-Rad FT175C FTIR equipped with a Ge/KBr beamsplitter and narrow band MCT detector. Spectral subtraction and curve fitting were performed using Grams/32 AI software (Galactic).

Acknowledgment

References

[1] J.-F. Capon, F. Gloaguen, P. Schollhammer, J. Talarmin, Coord. Chem. Rev. 249 (2005) 1664.

[2] S.J. Borg, T. Behrsing, S.P. Best, M. Razavet, X. Liu, C.J. Pickett, J. Am. Chem. Soc. 126 (2004) 16988.

[3] S.J. Borg, M.I. Bondin, S.P. Best, M. Razavet, X. Liu, C.J. Pickett, Biochem. Soc. Trans. 33 (2005) 3.

[4] M.H. Cheah, S.J. Borg, S.P. Best, Inorg. Chem. 46 (2007) 1741.

[5] C. Greco, G. Zampella, L. Bertini, M. Bruschi, P. Fantucci, L.D. Gioia, Inorg. Chem. 47 (2007) 108.

[6] M.H. Cheah, S.J. Borg, M.I. Bondin, S.P. Best, Inorg. Chem. 43 (2004) 5635.

[7] D. Chong, I.P. Georgakaki, R. Mejia-Rodriguez, J. Sanabria-Chinchilla, M.P. Soriaga, M.Y. Darensbourg, J. Chem. Soc., Dalton Trans. (2003) 4158.

[8] J.-F. Capon, F. Gloaguen, P. Schollhammer, J. Talarmin, J. Electroanal. Chem. 566 (2004) 241.

[9] J.-F. Capon, F. Gloaguen, P. Schollhammer, J. Talarmin, J. Electroanal. Chem. 595 (2006) 47.

[10] G.A.N. Felton, A.K. Vannucci, J. Chen, L.T. Lockett, N. Okumura, B.J. Petro, U.I. Zakai, D.H. Evans, R.S. Glass, D.L. Lichtenberger, J. Am. Chem. Soc. 129 (2007) 12521.

[11] G.A.N. Felton, R.S. Glass, D.L. Lichtenberger, D.H. Evans, Inorg. Chem. 45 (2006) 9181.

[12] T. Liu, M. Wang, Z. Shi, H. Cui, W. Dong, J. Chen, B. Akermark, L. Sun, Chem.—Eur. J. 10 (2004) 4474.

[13] J.W. Tye, J. Lee, H.-W. Wang, R. Mejia-Rodriguez, J.H. Reibenspies, M.B. Hall, M.Y. Darensbourg, Inorg. Chem. 44 (2005) 5550.

[14] L.-C. Song, Z.-Y. Yang, H.-Z. Bian, Y. Liu, H.-T. Wang, X.-F. Liu, Q.-M. Hu, Organometallics 24 (2005) 6126.

[15] Y. Na, M. Wang, K. Jin, R. Zhang, L. Sun, J. Organomet. Chem. 691 (2006) 5045.

[16] W. Dong, M. Wang, T. Liu, X. Liu, K. Jin, L. Sun, J. Inorg. Biochem. 101 (2007) 506.

[17] L. Duan, M. Wang, P. Li, Y. Na, N. Wang, L. Sun, J. Chem. Soc., Dalton Trans. (2007) 1277.

[18] Z. Wang, J. Liu, C. He, S. Jiang, B. Akermark, L. Sun, Inorg. Chim. Acta 360 (2007) 2411.

[19] K. Izutsu, Acid—Base Dissociation Constants in Dipolar Aprotic Solvents, Blackwell Scientific Publications, Oxford, 1990.

[20] A. Darchen, H. Mousser, H. Patin, J. Chem. Soc., Chem. Commun. (1988) 968.

[21] R. Mathieu, R. Poilblanc, P. Lemoine, M. Gross, J. Organomet. Chem. 165 (1979) 243.

[22] I. Aguirre de Carcer, A. Di Pasquale, A.L. Rheingold, D.M. Heinekey, Inorg. Chem. 45 (2006) 8000.

[23] S.P. Best, S.J. Borg, J.M. White, M. Razavet, C.J. Pickett, J. Chem. Soc., Chem. Commun. (2007) 4348.

[24] B. Rauchfuss Thomas, Inorg. Chem. 43 (2004) 14.

[25] E.J. Lyon, I.P. Georgakaki, J.H. Reibenspies, M.Y. Darensbourg, Angew. Chem., Int. Ed. 38 (1999) 3178.

[26] S.J. Borg, J.W. Tye, M.B. Hall, S.P. Best, Inorg. Chem. 46 (2007) 384.

[27] J.-F. Capon, S. Ezzaher, F. Gloaguen, F.Y. Petillon, P. Schollhammer, J. Talarmin, T.J. Davin, J.E. McGrady, K.W. Muir, New J. Chem. 31 (2007) 2052.

[28] S.J. Borg, Redox Interconversion Chemistry of Diiron Carbonyl Complexes, Ph.D. Thesis, University of Melbourne, Melbourne, 2005.

[29] K.A. Vincent, Elucidation of the Chemistry of FeMoco, Ph.D. Thesis, University of Melbourne, Melbourne, 2002.

[30] D.J. Curran, P.B. Graham, M.D. Rausch, Organometallics 12 (1993) 2380.

[31] E.J. Lyon, I.P. Georgakaki, J.H. Reibenspies, M.Y. Darensbourg, J. Am. Chem. Soc. 123 (2001) 3268.

[32] R.J. Errington, Guide to Practical Inorganic and Organo-Metallic Chemistry, Blackie Academic & Professional, London, 1997.

[33] D.T. Sawyer, A. Sobkowiak, J.J.L. Roberts, Electrochemistry for Chemists, second ed., Wiley-Interscience, New York, 1995.

[34] S.J. Borg, S.P. Best, J. Electroanal. Chem. 535 (2002) 57.

[35] D. Chang, T. Malinski, A. Ulman, K.M. Kadish, Inorg. Chem. 23 (1984) 817.

[36] N.G. Connelly, W.E. Geiger, Chem. Rev. 96 (1996) 877.

[37] M. Rudolph, in: I. Runinstein (Ed.), Physical Electrochemistry, CRC Press, Boca Raton, 1995, p. 81.

[38] M. Rudolph, J. Electroanal. Chem. 503 (2001) 15.

[39] M. Rudolph, J. Comput. Chem. 26 (2005) 1193.